Islamic Azad University

Journal of
Optoelectronical Nanostructures

Summer 2024 / Vol. 9, No. 3

Research Paper

FDTD Analysis of a High-Sensitivity Refractive Index Sensing Based on Fano Resonances in A Plasmonic Planar Split-Ring Resonators

Mohsen Nasrolahi [1], Ali Farmani*[2], Ashkan Horri[1] , Hossein Hatami[2]
[1] Department of Electrical Engineering, Islamic Azad University, Arak, Iran
[2] Department of Electrical Engineering, Lorestan University, Khoramabad, Iran

Received: 19 Feb. 2024
Revised: 20 Mar. 2024
Accepted: 1 Jun. 2024
Published: 15 Sep. 2024

Keywords:
Ring resonator, Plasmonics sensor, FDTD

Abstract

A tunable label-free refractive index biosensor based on plasmonic planar split-ring resonators is proposed. The effects of Fano resonances are studied to harness the transmission spectra in near-infrared region. In the structure, dual hexagonal ring resonators are utilized to realize the Fano resonances with the advantages of high sensitivity, large figure of merit, narrow full wave at half-maximum (FWHM), and extremely large Q-factor. Analytical and numerical outcomes display that, by slight variation of the refractive index and geometrical modes resonances can be manipulated. A high sensitivity of 1160 nm/RIU with a FoM as large as 33 is achieved. Besides, the proposed biosensor shows a relatively narrow FWHM of 50 nm, which introduces a high Q-factor of 31. Such this moderately high Q-factor ensures that the structure exhibits extreme low resonance losses that can be advantageous for high resolution detections with acceptable accuracy. Nano Fano resonance sensing is a technique used in nanophotonics for highly sensitive detection of bioanalytes. It leverages the Fano resonance effect, which arises from interference between a discrete state and a broadband continuum of states. This can lead to sharp asymmetric peaks in the absorption or scattering spectrum.

Citation: Mohsen Nasrolahi, Ali Farmani, Ashkan Horri, Hossein Hatami. FDTD Analysis of a High-sensitivity refractive index sensing based on Fano resonances in a plasmonic planar split-ring resonators. **Journal of Optoelectronical Nanostructures. 2024; 9 (3): 97-115. DOI:** 10.30495/JOPN.2024.33499.1321

***Corresponding author:** Ali Farmani
Address: Department of Electrical Engineering, Lorestan University, Khoramabad, Iran.
Tell: 00989355568142 **Email:** farmani.a@lu.ac.ir

1. INTRODUCTION

Numerous studies have explored various advancements in different types of biosensors, including unstable wave fluorescence sensors, photonic crystals, and surface plasmon resonance (SPR) sensors, with some of these studies focusing on specific applications. Optical biosensors have been highly welcomed by scientists in the last few years due to their fast response, small dimensions, low cost, timely detection ability, and ability to adapt to biological analytes with excellent s (sensitivity) and QF (quality factor). Taken in optical biosensors, a converter that converts the light change received from the source into measurable parameters is used to investigate the properties of the biological analyte for detection [1-6]. Usually, the measured parameters of the molecule are converted into measurable parameters such as intensity or wavelength resonance by a transducer [7-16]. The sensitivity value of the sensor is related to the architecture of the transducer and the waveguide structure used for measurement [16-23]. Optical biosensors have attracted the attention of researchers due to their small size and ability to be integrated, the cost of manufacturing and proper operation, and the detection of biological analyte without the need of any label [24-30]. Biosensors with resonator ring structure have smaller volume, better sensitivity and higher quality factor than photonic sensors such as photonic crystal, disk resonator sensors, MZI (Mach-Zehnder Interferometer) based sensors, PCF (photonic crystal fiber) sensors. [31-36]. Most plasmonic devices use metal-insulator-metal (MIM) waveguides for propagation [37-41], because MIM has the advantages of high sensitivity, ease of design, simple fabrication, and small dimensions. The most common metals used in these devices are the noble metals gold and silver, which have little losses in terms of ohmic [42-48]. However, they have a large optical wavelength penalty due to the energy required for interband transfer, intraband transfer, and scattered wave [49, 50]. Diffusion losses due to metallic nature are high and can cause errors in analyte detection. The response of the sensors that use the Kericthman configuration is good, but they are very expensive [51-54].

These elements may include antibodies, enzymes, proteins, and similar substances. Measurements are typically conducted by a transducer, followed by data analysis [55-60]. Optical biosensors are unique due to their use of optical measurement methods. These sensors utilize optical transducers to perform measurements, with the optical transducer closely integrated with the biosensing element.

For this reason, the classification of optical biosensors based on the type of

transducers is of great importance. One common approach in this classification is to divide them into two categories: labeled and unlabeled. In labeled biosensors, fluorescent or chromogenic markers are used, where the intensity of fluorescence or color change is analyzed for the identification of analytes [60-64].

Here, with Finite-Difference Time-Domain (FDTD) a novel biosensor is suggested.

Taken together, the proposed plasmonic biosensor might pave the way towards the related limitations of biosensing, detection, and imaging.

2. THEORY OF SCHOTTKY JUNCTION

Ring resonators have many uses due to their ability to be integrated and have been noticed and have emerged in integrated optics. Integrated ring resonators do not need a periodic surface under the wave or a mirror and a prism or grating surface for optical feedback. As a result, their structure is small and can be integrated. be made with other components. In the design of ring resonators, their structure can be customized and coupled in different ways. Thus, plasmonic biosensors constructed with label-free ring resonators that operate based on changes in the refractive index parameter can be widely used in medical applications, imaging, disease diagnosis, and pathogens in various foods. be placed.

The basic design includes a one-way resonator ring, we show the ring radius with r and the width of the waveguide with a that in one direction, the coupling and excitation mode is created in the resonator, in this case the loss is very small and we consider it as zero. The polarization has been investigated individually so that the coupling between the ring and the waveguide of different polarizations does not occur. Different losses occur along the propagation path. Resonance mode occurs at a specific wavelength and frequency, and the coupling of light occurs in the ring (see Figure 1.).

 DOI: 10.30495/JOPN.2024.33499.1321

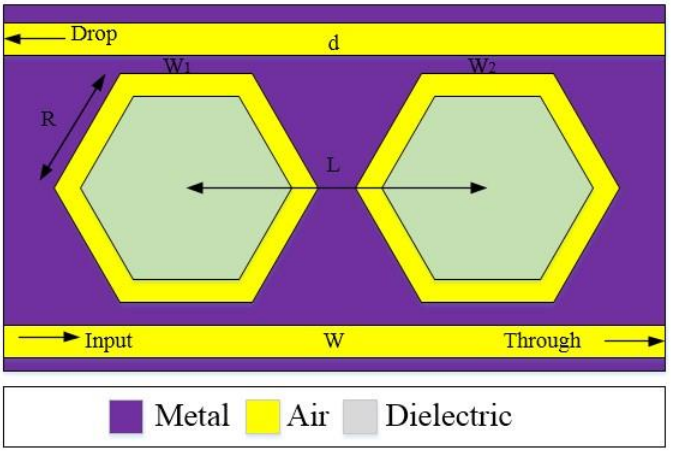

Fig. 1 2D-configuration of biosensor

A part of the structure illustrates in the following figure.

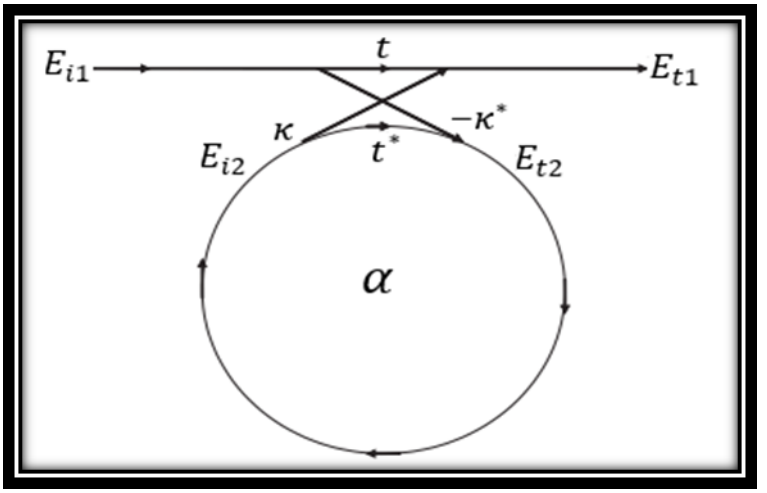

Fig. 2 Fano resonance structure

For analysis, we can express the relationship between input and output by considering the attenuation coefficient of the light path as follows:

$$\begin{pmatrix} E_{t1} \\ E_{t2} \end{pmatrix} = \begin{pmatrix} t & \kappa \\ -\kappa^* & t^* \end{pmatrix} \begin{pmatrix} E_{i1} \\ E_{i2} \end{pmatrix} \quad (1)$$

For the simplicity of the analysis of mixed modes, we normalize E, in this case, the absolute value of their square is equal to the modal power. We represent the path length attenuation coefficient with t and the coupling attenuation coefficient with k. With this interpretation, we have:

$$|\kappa^2| + |t^2| = 1 \quad (2)$$

To simplify the analysis model, we consider E_{i1} equal to 1. Therefore, the circular path is defined by the following relation:

$$E_{i2} = \alpha \cdot e^{j\theta} E_{t2} \quad (3)$$

Considering that α is the attenuation coefficient of the loop, for zero loss mode, we should consider it equal to 1 (α = 1). The position angle θ is defined according to the relation (θ=ωL/c), in this relation L is the circumference of the ring and r is the radius of the ring. So L = 2πr. c is the phase speed that is related to the speed of light in vacuum and the effective refractive index according to the state (c=c0/"neff"). Also, ω is the angular frequency that is related to the speed of light in vacuum c0 and the wave number k according to ω = kc0. The vacuum wave number k depends on the wavelength λ, k = 2π/λ. Therefore, we can write the relations as follows:

$$\beta = k \cdot n_{\text{eff}} = \frac{2\pi \cdot n_{\text{eff}}}{\lambda} \quad (4)$$

Considering that β is the propagation constant, we have:

$$\theta = \frac{\omega L}{c} = \frac{k c_0 L}{c} = k \cdot n_{\text{eff}} \cdot 2\pi r = \frac{2\pi \cdot n_{\text{eff}} \cdot 2\pi r}{\lambda} = 4\pi^2 n_{\text{eff}} \frac{r}{\lambda} \quad (5)$$

From (1) and (3) we get:

$$E_{t1} = \frac{-\alpha + t \cdot e^{-j\theta}}{-\alpha t^* + e^{-j\theta}} \quad (6)$$

$$E_{t1} = \frac{-\alpha + t \cdot e^{-j\theta}}{-\alpha t^* + e^{-j\theta}} \quad (7)$$

$$E_{i2} = \frac{-\alpha \kappa^*}{-\alpha t^* + e^{-j\theta}} \quad (8)$$

As a result, we can obtain the output power according to the following equation:

$$P_{t_1} = |E_{t_1}|^2 = \frac{\alpha^2 + |t|^2 - 2\alpha|t| \cos(\theta + \varphi_t)}{1 + \alpha^2|t|^2 - 2\alpha|t| \cos(\theta + \varphi_t)} \quad (9)$$

The coupling loss can be obtained from the relation t = |t| exp (jϕt) obtained, as previously stated |t| Coupling loss and φ_t is the coupling phase. Therefore, we get the power $P_{i\gamma}$ in the loop as follows:

$$P_{t_2} = |E_{t_2}|^2 = \frac{\alpha^2(1 - |t|^2)}{1 + \alpha^2|t|^2 - 2\alpha|t| \cos(\theta + \varphi_t)} \quad (10)$$

In the intensified state, we have the relation , $(\theta+\varphi_t)=2\pi m$. Note that m is an integer, so the relations are simplified as follows:

$$P_{t_1} = |E_{t_1}|^2 = \frac{(\alpha - |t|)^2}{(1 - \alpha|t|)^2} \quad (11)$$

$$P_{t_2} = \left|E_{t_2}\right|^2 = \frac{\alpha^2(1-|t|)^2}{(1-\alpha|t|)^2} \quad (12)$$

In a special case where the internal loss of the resonator ring is equal to the coupling loss, i.e.,

$\alpha = |t|$, the transmission power becomes zero. This is the critical coupling state. The equations mentioned for a ring and a waveguide are a good model for other resonator ring configurations. And it can be used to analyze the complex structures of the resonator ring

The Sensitivity (S) is defined as:

$$S = \frac{\Delta\lambda}{\Delta n} \quad (13)$$

FoM is expressed as:

$$FoM = \frac{S}{FWHM} \quad (14)$$

Integrated resonators with high Q-factors are highly desirable because plasmonic biosensor with high Q, suggest narrower FWHM, high FoM, low resonator losses and large sensitivity. The Q-factor is defined as [61]:

$$Q = \frac{\lambda_{res}}{FWHM} \quad (15)$$

Where λ_{res} is the wavelength in which the spectral slope reaches its maximum.

3. Results and Discussions

In this section, the Fano resonance is observed through modulation of geometric parameters and variation of refractive indices.

3.1 Numerical Results

Here, the resonances are defined as FR1 and FR2. For FR1, T_{max} occurs at $\lambda_{peak} = 630nm$ and T_{max} occurs at $\lambda_{dip} = 780nm$. Therefore, the FWHM for FR1 can be calculated as 150 nm. Similarly, for FR2, T_{max} and and T_{min} occur at $\lambda_{peak} = 640nm$ and $\lambda_{dip} = 740nm$, respectively. As a result, the FWHM for FR2 is 100 nm. Additionally, it can be seen that in the range of 650 - 850 nm, there are two

symmetric Lorentzian like valleys which represent the first and the second eigen mode of the ring cavity (see Fig.3).

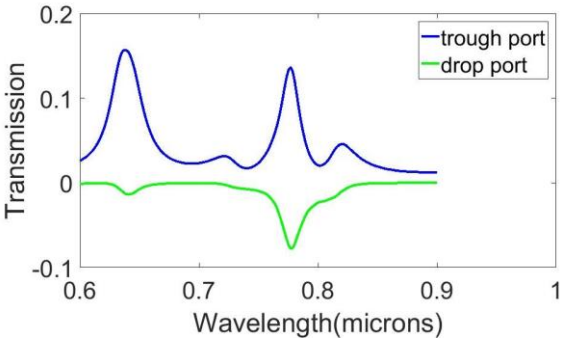

Fig. 3 The transmission of two Fano resonance

Physical analysis of the structure of the resonator ring is very important in order to achieve how the resonator ring works and requires complex mathematical operations. One of the methods of numerical analysis of instruments is Finite Difference Time Domain (FDTD) and it can perform analysis in the time domain as well. Therefore, it is perfect for the resonator loop and provides a very good view. We have presented a biosensor with a hybrid structure of plasmonic resonator ring along with modeling and numerical analysis. This hybrid structure based on highly doped n-graphene silicon waveguide is very suitable for biosensor application. We have proposed this new structure based on the research and investigation of different structures and different plasmonic devices according to the following findings to improve and improve the functional parameters of the biosensor.

A- The use of the ring structure of integrated resonators because they do not need a periodic surface under the wave or a mirror and a prism surface or a net for optical feedback. As a result, their structure is small and they can be made as a complex with other components.

B- We have used the hybrid structure of two lines of resonator ring. The use of degenerate semiconductor due to high doping, which reduces losses compared to noble conductors such as gold and silver, and because it is more compatible with CMOS integration technology.

C- Adding a layer of graphene to the structure, in fact, graphene is used to detect various types of organic and inorganic substances in biological and environmental applications, including glucose, cysteine, proteins, biological

markers, DNA, heavy metals, etc. Also, biosensors in which graphene is used have been used for early detection of various diseases and cancers.

In order to achieve better parameters of the biosensor and improve the performance, we have taken the help of the gray wolf algorithm, and we have done the modeling using the FDTD method.

Optimization problems are ubiquitous across various domains, spanning single or multiple objectives and often characterized by intricate landscapes of high dimensionality. Traditional optimization methodologies frequently encounter limitations when confronted with such complexities. In response, metaheuristic algorithms have emerged as promising alternatives, drawing inspiration from natural or social systems to navigate complex problem spaces effectively. The field profile display in Fig.4.

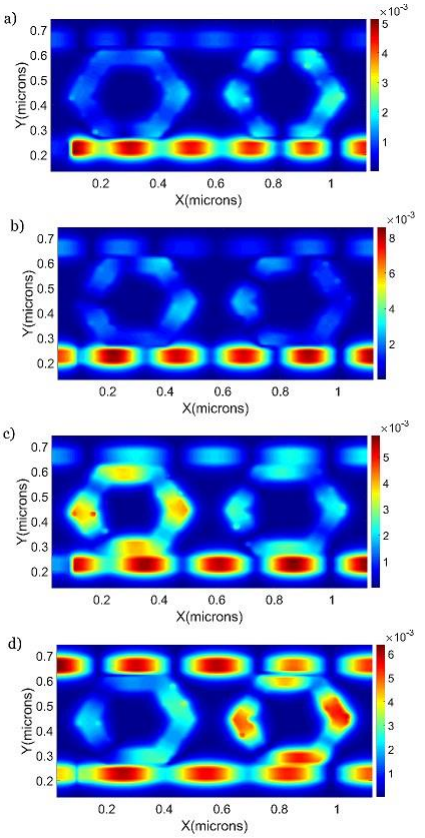

Fig. 4 Demonstration of Fano resonance, FR1 and FR2, using magnetic field distributions ($|H_z|$) at (630 nm (a), 780 nm (c)) and (640 nm (b), 740 nm (d))

The effects of different noble metals display in Fig.5.

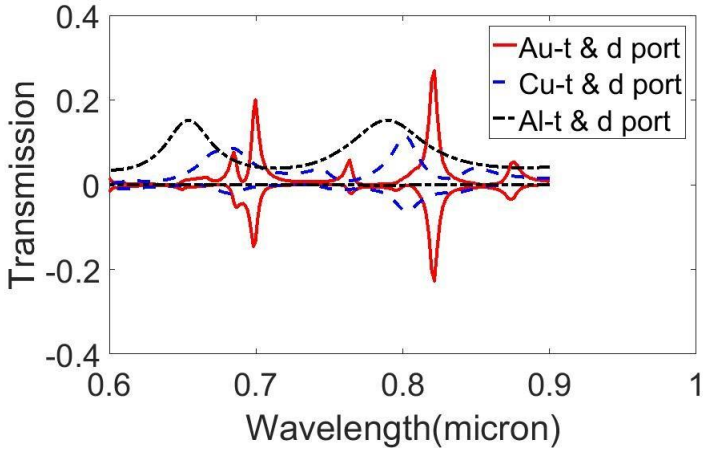

Fig. 5 The transmission of different noble metals.

As injected light comes from two through and drop ports. Inverse behavior of these ports calculated in Fig.6.

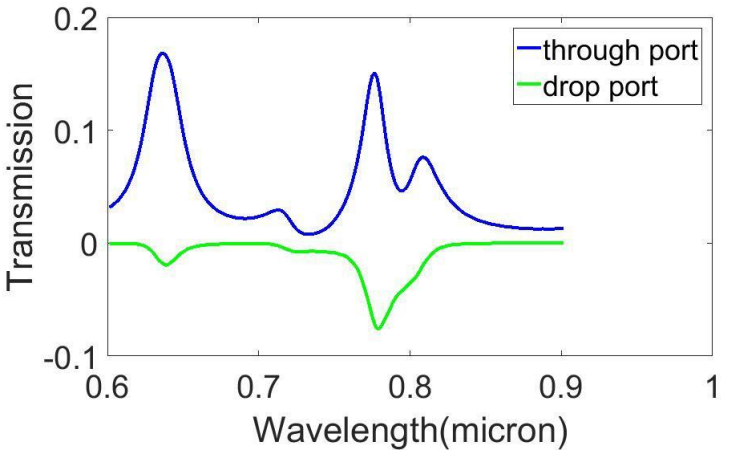

Fig. 6 The transmission in through and drop ports

when the thickness of the metal waveguide increases (see Fig. 7 (b)), the continua state is almost disappeared, and the transmission spectrum takes on a symmetric Lorentzian linestyle. The above characteristics indicate that we can tune the Fano resonance by changing the thickness of the metal waveguide.

3.2 Refractive index sensing

Refractive index sensing is a technique used to measure the refractive index of a substance, which is a dimensionless value that describes how light propagates through that substance. It is commonly used in various fields including chemistry, biology, and physics for applications such as detecting biomolecules, monitoring chemical reactions, and studying materials properties. The principle behind refractive index sensing is based on the fact that the speed of light changes as it passes through different mediums with varying refractive index. The effect of various L plots in Fig.7.

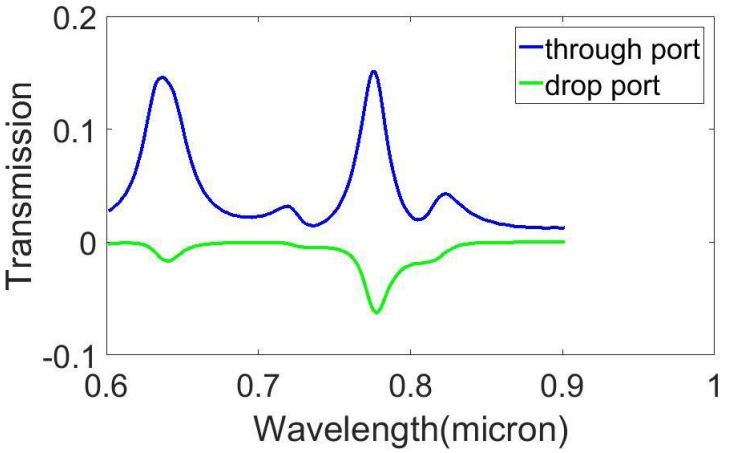

Fig. 7 The effect of L_1.

Comparison Table is provided (see Table 1). In this realm some valuable works are presented [68-70].

Table 2 benchmark of the work.

Refrence	Frequency range	Sensitivity	Structure	Footprint (nm×nm×nm)
Zhang [65]	Near infrared	1060	MIM Waveguide	800 × 800 × 1000
Zafar [66]	Near infrared	1100	MIM Waveguide	>400 × >1000 × >1000
Zafar [67]	Near infrared	–	Split-Ring Metasurface	700 × 700 × 110
This Work	Visible	1160	Split-ring resonator	700 × 1000 × 100

4. CONCLUSION

Here, Fano resonance in plasmonic planar split-ring resonators, a tunable refractive index biosensor is proposed. It was shown variation of refractive indices leads to various exited modes. Such sharpness is an indication of narrow FWHM with the value of 50 nm, which in turn translates into high sensitivity as high as 1160 nm/RIU with large FoM of 33. Furthermore, thanks to the introduction of hexagonal resonators coupled with the Fano effects, the biosensor demonstrated extremely high Q-factor as large as 31 at the resonant wavelength of 740 nm. This, apparently, leads to small resonant losses and high integration which can be undoubtedly beneficial for a biosensor. Fano resonance sensing is an important application in the field of photonics and plasmonics. It involves detecting tiny changes in the environment or material properties by studying the asymmetric lineshape of Fano resonances. This technique is often used in sensor technology for detecting small variations in refractive index, temperature, pressure, or molecular interactions

ACKNOWLEDGMENT

This work was supported by Lorestan University.

REFERENCES

[1] Barnes, William L., Alain Dereux, and Thomas W. Ebbesen. "*Surface plasmon subwavelength optics*." nature 424.6950 (2003): 824-830. Available: https://doi.org/10.1038/nature01937.

[2] Wu, Wenjun, et al. "*Ultra-high resolution filter and optical field modulator based on a surface plasmon polariton*." Optics letters 41.10 (2016): 2310-2313.Available: https://doi.org/10.1364/OL.41.002310

[3] Wu, Dong, et al. "*Numerical study of an ultra-broadband near-perfect solar absorber in the visible and near-infrared region*." Optics letters 42.3 (2017): 450-453.Available: https://doi.org/10.1364/OL.42.000450

[4] Yu, Yue, et al. "*Plasmonic wavelength splitter based on a metal–insulator–metal waveguide with a graded grating coupler*." Optics letters 42.2 (2017): 187-190. https://doi.org/10.1364/OL.42.000187

[5] Chen, Lei, et al. "*Numerical analysis of a near-infrared plasmonic refractive index sensor with high figure of merit based on a fillet cavity*." Optics express 24.9 (2016): 9975-9983.Available: https://doi.org/10.1364/OE.24.009975

[6] Shen, Yang, et al. "*Plasmonic gold mushroom arrays with refractive index sensing figures of merit approaching the theoretical limit*." Nature communications 4.1 (2013): 2381, Available: https://doi.org/10.1038/ncomms3381

[7] Srivastava, Triranjita, Ritwick Das, and Rajan Jha. "*Highly sensitive plasmonic temperature sensor based on photonic crystal surface plasmon waveguide*." Plasmonics 8 (2013): 515-521.Available:

https://doi.org/10.1007/s11468-012-9421-x

[8] Maisonneuve, M., et al. "*Phase sensitive sensor on plasmonic nanograting structures*." Optics express 19.27 (2011): 26318-26324.Available: https://doi.org/10.1364/OE.19.026318

[9]Elsayed, Mohamed Y., Yehea Ismail, and Mohamed A. Swillam. "*Semiconductor plasmonic gas sensor using on-chip infrared spectroscopy*." Applied Physics A 123.1 (2017): 113.Available: https://doi.org/10.1007/s00339-016-0707-2

[10] Rosenzveig, Tiberiu, Petur G. Hermannsson, and Kristjan Leosson.

"*Modelling of polarization-dependent loss in plasmonic nanowire waveguides*." Plasmonics 5 (2010): 75-77.Available: https://doi.org/10.1007/s11468-009-9118-y

[11] Zhang, Zhongyue, et al. "*Numerical investigation of a branch-shaped filter based on metal-insulator-metal waveguide*." Plasmonics 6 (2011): 773-778., Available: https://doi.org/10.1007/s11468-011-9263-y

[12] Wei, Hong, et al. "*Directionally-controlled periodic collimated beams of surface plasmon polaritons on metal film in Ag nanowire/Al2O3/Ag film composite structure*." Nano Letters 15.1 (2015): 560-564.Available: https://doi.org/10.1021/nl504018q

[13] Chen, Chyong-Hua, and Kao-Sung Liao. "*1xN plasmonic power splitters based on metal-insulator-metal waveguides.*" Optics express 21.4 (2013): 4036-4043.Available: https://doi.org/10.1364/OE.21.004036

[14] Chen, Zhao, et al. "*Plasmonic wavelength demultiplexers based on tunable Fano resonance in coupled-resonator systems*." Optics Communications 320 (2014): 6-11.Available: https://doi.org/10.1016/j.optcom.2013.12.079

[15] Chen, Li, et al. "*A subwavelength MIM waveguide filter with single-cavity and multi-cavity structures*." Optik-International Journal for Light and Electron Optics 124.18 (2013): 3701-3704., Available: https://doi.org/10.1016/j.ijleo.2012.11.025

[16] Wu, Tiesheng, et al. "*The sensing characteristics of plasmonic waveguide with a ring resonator*." Optics express 22.7 (2014): 7669-7677.Available: https://doi.org/10.1364/OE.22.007669

[17] Lodewijks, Kristof, et al. "*Tuning the Fano resonance between localized and propagating surface plasmon resonances for refractive index sensing applications*." Plasmonics 8 (2013): 1379-1385.Available: https://doi.org/10.1007/s11468-013-9549-3

[18] Francescato, Yan, Vincenzo Giannini, and Stefan A. Maier. "*Plasmonic systems unveiled by Fano resonances.*" ACS nano 6.2 (2012): 1830-1838.Available: https://doi.org/10.1021/nn2050533

[19] Hao, Feng, et al. "*Tunability of subradiant dipolar and Fano-type plasmon resonances in metallic ring/disk cavities: implications for nanoscale optical sensing.*" ACS nano 3.3 (2009): 643-652.,Available: https://doi.org/10.1021/nn900012r

[20] Rybin, Mikhail V., et al. "*Fano resonances in antennas: General control over radiation patterns*." Physical Review B—Condensed Matter and Materials Physics 88.20 (2013): 205106.Available: https://doi.org/10.1103/PhysRevB.88.205106

[21] Fan, Jonathan A., et al. "*Fano-like interference in self-assembled plasmonic quadrumer clusters*." Nano letters 10.11 (2010): 4680-4685.Available: https://doi.org/10.1021/nl1029732

[22] Fano, Ugo. "*Effects of configuration interaction on intensities and phase shifts."* Physical review 124.6 (1961): 1866.Available: https://doi.org/10.1103/PhysRev.124.1866

[23] Zhang, Shunping, et al. "*Reduced linewidth multipolar plasmon resonances in metal nanorods and related applications."* Nanoscale 5.15 (2013): 6985-6991. Available: https://doi.org/10.1039/C3NR01219K

[24] Gallinet, Benjamin, and Olivier JF Martin. "*Refractive index sensing with subradiant modes: a framework to reduce losses in plasmonic nanostructures*." ACS nano 7.8 (2013): 6978-6987.Available: https://doi.org/10.1021/nn4021967

[25] Prodan, Emil, et al. "*A hybridization model for the plasmon response of complex nanostructures*." science 302.5644 (2003): 419-422.Available: 10.1126/science.1089171

[26] Wang, H. U. I., et al. "*Plasmonic nanostructures: artificial molecules*." Accounts of chemical research 40.1 (2007): 53-62.Available: https://doi.org/10.1021/ar0401045

[27] D'Agostino, Stefania, Fabio Della Sala, and Lucio Claudio Andreani. "*Radiative coupling of high-order plasmonic modes with far-field*." Photonics and Nanostructures-Fundamentals and Applications 11.4 (2013): 335-344.Available: https://doi.org/10.1016/j.photonics.2013.06.003

[28] Halas, Naomi J., et al. "*Plasmons in strongly coupled metallic nanostructures*." Chemical reviews 111.6 (2011): 3913-3961.Available: https://doi.org/10.1021/cr200061k

[29] Liu, Jui-Nung, et al. "*Resonant coupling from photonic crystal surfaces to plasmonic nanoantennas: principles, detection instruments, and applications in digital resolution biosensing.*" Smart Photonic and Optoelectronic Integrated Circuits XX. Vol. 10536. SPIE, 2018.Available:

https://doi.org/10.1117/12.2285828

[30] Miroshnichenko, Andrey E., Sergej Flach, and Yuri S. Kivshar. "*Fano resonances in nanoscale structures*." Reviews of Modern Physics 82.3 (2010): 2257-2298.Available: https://doi.org/10.1103/RevModPhys.82.2257

[31] Verellen, Niels, et al. "*Fano resonances in individual coherent plasmonic nanocavities*." Nano letters 9.4 (2009): 1663-1667.Available: https://doi.org/10.1021/nl9001876

[32] Sheikholeslami, Sassan, et al. "*Coupling of optical resonances in a compositionally asymmetric plasmonic nanoparticle dimer*." Nano letters 10.7 (2010): 2655-2660.Available: https://doi.org/10.1021/nl101380f

[33] Mukherjee, Shaunak, et al. "*Fanoshells: nanoparticles with built-in Fano resonances*." Nano letters 10.7 (2010): 2694-2701.Available: https://doi.org/10.1021/nl1016392

[34] Y." Sonnefraud, N. Verellen, H. Sobhani, GA E. Vandenbosch, VV Moshchalkov, *P. Van Dorpe, P. Nordlander, and S. A. Maier*, ibid 4 (2010): 1664.

[35] Chu, Ming-Wen, et al. "*Probing bright and dark surface-plasmon modes in individual and coupled noble metal nanoparticles using an electron beam*." Nano letters 9.1 (2009): 399-404.Available: https://doi.org/10.1021/nl803270x

[36] Firoozi, A., Khordad, R., & Rastegar Sedehi, H. R. (2023). *Modelling of nanosensors based on localised surface plasmon resonance*. Philosophical Magazine, 103(22), 2054-2071., Available: https://doi.org/10.1080/14786435.2023.2255143

[37] Yang, Shu-Chun, et al. "*Plasmon hybridization in individual gold nanocrystal dimers: direct observation of bright and dark modes*." Nano letters 10.2 (2010): 632-637.Available: https://doi.org/10.1021/nl903693v

[38] Firoozi, A., Amphawan, A., Khordad, R., Mohammadi, A., Jalali, T., Edet, C. O., & Ali, N. (2023). *Effect of nanoshell geometries, sizes, and quantum emitter parameters on the sensitivity of plasmon-exciton hybrid nanoshells for sensing application*. Scientific Reports, 13(1), 11325. Available: https://doi.org/10.1038/s41598-023-38475-1

[39] Firoozi, A., Khordad, R., & Rastegar Sedehi, H. R. (2024). *Study of*

enhanced sensitivity of nanosensors by using gold bowtie nanoparticles. Journal of Nonlinear Optical Physics & Materials, 33(05), 2350057. Available: https://doi.org/10.1142/S0218863523500571

[40] Dehghani, M., Hatami, M., & Gharaati, A. (2021). *Research Paper Supercontinuum Generation in Silica Plasmonic Waveguide by Bright Soliton*. Journal of Optoelectronical Nanostructures, 6(4), 109-136. Available: 10.30495/JOPN.2022.28937.1236

[41] Mansuri, M., Mir, A., & Farmani, A. (2019). *Numerical modeling of a nanostructure gas sensor based on plasmonic effect*. Journal of Optoelectronical Nanostructures, 4(2), 29-44. Available: 20.1001.1.24237361.2019.4.2.3.3

[42] Farmani, A., Mir, A., & Sharifpour, Z. (2018). *Broadly tunable and bidirectional terahertz graphene plasmonic switch based on enhanced Goos-Hänchen effect*. Applied Surface Science, 453, 358-364. Available: https://doi.org/10.1016/j.apsusc.2018.05.092

[43] Farmani, A., Miri, M., & Sheikhi, M. H. (2017). *Tunable resonant Goos–Hänchen and Imbert–Fedorov shifts in total reflection of terahertz beams from graphene plasmonic metasurfaces*. JOSA B, 34(6), 1097-1106. Available: https://doi.org/10.1364/JOSAB.34.001097

[44] Farmani, A. (2019). *Three-dimensional FDTD analysis of a nanostructured plasmonic sensor in the near-infrared range*. JOSA B, 36(2), 401-407. Available: https://doi.org/10.1364/JOSAB.36.000401

[45] Farmani, A., Zarifkar, A., Sheikhi, M. H., & Miri, M. (2017). *Design of a tunable graphene plasmonic-on-white graphene switch at infrared range*. Superlattices and Microstructures, 112, 404-414. Available: https://doi.org/10.1016/j.spmi.2017.09.051

[46] Moradiani, F., Farmani, A., Mozaffari, M. H., Seifouri, M., & Abedi, K. (2020). *Systematic engineering of a nanostructure plasmonic sensing platform for ultrasensitive biomaterial detection*. Optics Communications, 474, 126178. Available: https://doi.org/10.1016/j.optcom.2020.126178

[47] Hamzavi-Zarghani, Z., Yahaghi, A., Matekovits, L., & Farmani, A. (2019). *Tunable mantle cloaking utilizing graphene metasurface for terahertz sensing applications*. Optics Express, 27(24), 34824-34837. Available:

https://doi.org/10.1364/OE.27.034824

[48] Amoosoltani, N., Zarifkar, A., & Farmani, A. (2019). *Particle swarm optimization and finite-difference time-domain (PSO/FDTD) algorithms for a surface plasmon resonance-based gas sensor*. Journal of Computational Electronics, 18, 1354-1364. Available: https://doi.org/10.1007/s10825-019-01391-7

[49] Sadeghi, T., Golmohammadi, S., Farmani, A., & Baghban, H. (2019). *Improving the performance of nanostructure multifunctional graphene plasmonic logic gates utilizing coupled-mode theory*. Applied Physics B, 125, 1-12. Available: https://doi.org/10.1007/s00340-019-7305-x

[50] Salehnezhad, Z., Soroosh, M., & Farmani, A. (2023). *Design and numerical simulation of a sensitive plasmonic-based nanosensor utilizing MoS2 monolayer and graphene*. Diamond and Related Materials, 131, 109594. Available: https://doi.org/10.1016/j.diamond.2022.109594

[51] Hamza, Musa N., et al. "*Development of a Terahertz Metamaterial Micro-Biosensor for Ultrasensitive Multispectral Detection of Early-Stage Cervical Cancer*." IEEE Sensors Journal (2024).Available: 10.1109/JSEN.2024.3447728

[52] Amoosoltani, N., Yasrebi, N., Farmani, A., & Zarifkar, A. (2020). *A plasmonic nano-biosensor based on two consecutive disk resonators and unidirectional reflectionless propagation effect*. IEEE Sensors Journal, 20(16), 9097-9104. Available: 10.1109/JSEN.2020.2987319

[53] Khajeh, A., Hamzavi-Zarghani, Z., Yahaghi, A., & Farmani, A. (2021). *Tunable broadband polarization converters based on coded graphene metasurfaces*. Scientific Reports, 11(1), 1296. Available: https://doi.org/10.1038/s41598-020-80493-w

[54] Khani, S., Farmani, A., & Mir, A. (2021). *Reconfigurable and scalable 2, 4-and 6-channel plasmonics demultiplexer utilizing symmetrical rectangular resonators containing silver nano-rod defects with FDTD method*. Scientific Reports, 11(1), 13628. Available: https://doi.org/10.1038/s41598-021-93167-y

[55] Moradiani, F., Farmani, A., Yavarian, M., Mir, A., & Behzadfar, F. (2020). *A multimode graphene plasmonic perfect absorber at terahertz frequencies*. Physica E: Low-dimensional Systems and Nanostructures, 122, 114159. Available:

https://doi.org/10.1016/j.physe.2020.114159

[56] Farmani, H., & Farmani, A. (2020). *Graphene sensing nanostructure for exact graphene layers identification at terahertz frequency*. Physica E: Low-dimensional Systems and Nanostructures, 124, 114375. Available: https://doi.org/10.1016/j.physe.2020.114375

[57] Fouladi, H., Farmani, A., & Mir, A. (2023). *Rigorous Investigation of Ring Resonator Nanostructure for Biosensors applications in breast cancer detection*. Journal of Optoelectronical Nanostructures, 8(4), 97-119. Available: 10.30495/JOPN.2024.32304.1299

[58] Hamza, Musa N., Mohammad Tariqul Islam, Slawomir Koziel, Muhamad A. Hamad, Iftikhar ud Din, Ali Farmani, Sunil Lavadiya, and Mohammad Alibakhshikenari. "*Designing a High-sensitivity Microscale Triple-band Biosensor based on Terahertz MTMs to provide a perfect absorber for Non-Melanoma Skin Cancer diagnostic*." IEEE Photonics Journal (2024). Available: 10.1109/JPHOT.2024.3381649

[59] Zangeneh, A. M. R., Farmani, A., Mozaffari, M. H., & Mir, A. (2022). *Enhanced sensing of terahertz surface plasmon polaritons in graphene/J-aggregate coupler using FDTD method*. Diamond and Related Materials, 125, 109005. Available: https://doi.org/10.1016/j.diamond.2022.109005

[60] M. Soroosh, A. Mirali, E. Farshidi. *Ultra-Fast All-Optical Half Subtractor Based on Photonic Crystal Ring Resonators*. Journal of Optoelectronical Nanostructures., 5(1) (2020) 83-100. Available: https://dorl.net/dor/20.1001.1.24237361.2020.5.1.6.1

[61] Khosravian, E., Mashayekhi, H. R., & Farmani, A. (2021). Highly *polarization-sensitive, broadband, low dark current, high responsivity graphene-based photodetector utilizing a metal nano-grating at telecommunication wavelengths*. JOSA B, 38(4), 1192-1199. Available: https://doi.org/10.1364/JOSAB.418804

[62] Jafrasteh, F., Farmani, A., & Mohamadi, J. (2023). *Meticulous research for design of plasmonics sensors for cancer detection and food contaminants analysis via machine learning and artificial intelligence*. Scientific Reports, 13(1), 15349. Available: https://doi.org/10.1038/s41598-023-42699-6

[63] Farmani, A., & Omidniaee, A. (2024). *Observation of Plasmonics Talbot effect in graphene nanostructures*. Scientific Reports, 14(1), 1973. Available: https://doi.org/10.1038/s41598-024-52595-2

[64] Mohammadi, M., Soroosh, M., Farmani, A., & Ajabi, S. (2023). *Engineered FWHM enhancement in plasmonic nanoresonators for multiplexer/demultiplexer in visible and NIR range*. Optik, 274, 170583. Available: https://doi.org/10.1016/j.ijleo.2023.170583

[65] X. Zhang, Y. Qi, P. Zhou, H. Gong, B. Hu, C. Yan, *Photonic Sensors* 8(4), 367 (2018) https://doi.org/10.1007/s13320-018-0509-6

[66] R. Zafar, M. Salim, *IEEE Sensors Journal* 15(11), 6313 (2015) Available: 10.1109/JSEN.2015.2455534

[67] R. Zafar, S. Nawaz, G. Singh, A. d'Alessandro, M. Salim, *IEEE Sensors Journal* (2018) Available: 10.1109/JSEN.2018.2826040

[68] F. Pakrai, M. Soroosh, and J. Ganji. *Designing of all-optical subtractor via PC-based resonators*. Journal of Optoelectronical Nanostructures., 7(2) (2022) 21-36. Available: https://doi.org/10.30495/JOPN.2022.29545.1246

[69] B. Elyasi and S. Javahernia. *All optical digital multiplexer using nonlinear photonic crystal ring resonators.* Journal of Optoelectronical Nanostructures., 7(1) (2022) 97-106. Available: https://doi.org/10.30495/jopn.2022.29174.1242

[70] F. Khatib and M. Shahi. *Ultra-Fast All-Optical Symmetry 4×2 Encoder Based on Interface Effect in 2D Photonic Crystal*. Journal of Optoelectronical Nanostructures., 5(3) (2020) 103-114. Available: https://dorl.net/dor/20.1001.1.24237361.2020.5.3.7.6